PHYSICAL REVIEW B VOLUME 44, NUMBER 17 1 NOVEMBER 1991-I

Evidence of quadrupolar scattering in the anisotropic electrical magnetoresistivity of $PrNi_5$

J. A. Blanco*
Laboratoire Louis Néel, CNRS, 166X, 38042, Grenoble CEDEX, France

M. Reiffers
Institute of Experimental Physics, Slovakian Academy of Sciences, 04353 Kosice, Czechoslovakia

D. Gignoux and D. Schmitt
Laboratoire Louis Néel, CNRS, 166X, 38042, Grenoble CEDEX, France

A. G. M. Jansen
Max-Plank-Institut für Festkörperforschung Hochfeld-Magnetlabor, 166X, 38042 Grenoble CEDEX, France
(Received 6 February 1991)

The temperature and magnetic-field dependences of the electrical resistivity measured on a single crystal of the Van Vleck paramagnetic $PrNi_5$ exhibit an anisotropic behavior. The influence of the spin-disorder scattering as well as the quadrupolar scattering of conduction electrons by the $4f$ shell must be taken into account to explain the experimental results. In particular, a quadrupolar contribution plays an important role in the observed anisotropy.

I. INTRODUCTION

It is well known that the $4f$ electrons of rare-earth ions having $L \neq 0$ carry not only a magnetic dipolar, but also a quadrupolar moment. This can give rise to an additional contribution to the conventional part of the electrical resistivity, which is expected to be anisotropic as a result of the aspherical $4f$ charge distribution. Initially, this quadrupolar contribution was studied in cubic noble metals containing rare-earth impurities.[1,2] An anisotropic behavior of the electrical magnetoresistivity of polycrystalline samples was observed through the influence of the magnetic-field orientation with respect to the electrical-current orientation on the resistivity (so-called longitudinal and transverse magnetoresistivity). Later, in the ferromagnetic $PrAl_2$ cubic compound a "spontaneous anisotropy" of the electrical resistivity below the transition temperature T_c associated with a symmetry lowering has been observed.[3] In this case the anisotropic quadrupolar scattering was smaller than the isotropic one. Thus one can also expect for systems with axial symmetry, where there exists a spontaneous aspherical distribution of $4f$ charges, a noticeable influence of the anisotropic quadrupolar contribution to the magnetoresistivity.

To our knowledge few experiments have been devoted to this situation. Therefore, we have undertaken magnetoresistivity measurements on a system with hexagonal symmetry, namely, $PrNi_5$.

$PrNi_5$ is a very interesting system which has been extensively studied. Although bilinear exchange interactions are present, they are undercritical to induce a $4f$ magnetic order in this system because of the existence of a crystalline electrical-field (CEF) singlet ground state.[4,5] The previous experiments showed that all the properties of $PrNi_5$ are strongly influenced by CEF. The temperature dependence of the electrical resistivity of a $PrNi_5$ polycrystalline sample has been measured at low temperatures, and the experimental results could be satisfactorily fitted up to 15 K by the spin-disorder resistivity (SDR) model.[16] However, this model has given only a qualitative explanation of the electrical magnetoresistivity dependences obtained on this sample under magnetic fields up to 7 T.[7]

On the other hand, the magnetic properties of the $PrNi_5$ compound are quite well understood. The influence of the quadrupolar moment on the magnetic and magnetoelastic properties allowed us to determine the magnetoelastic coefficients and total quadrupolar coefficients G^{α} and G^{ε}, leading to the experimental evidence of antiferroquadrupolar interactions between rare-earth ions.[8]

More recently, direct measurement of the anisotropic Zeeman splitting of the CEF levels, in magnetic fields up to 22 T, has been performed by point-contact spectroscopy.[9] The interpretation of the experiment led to a slight adjustment of the CEF parameters so that they account better for the position of the first excited CEF level observed by this technique in a magnetic field.

In order to study the possible anisotropy of the electrical magnetoresistivity on a single crystal of $PrNi_5$, we have measured the temperature and magnetic-field dependences of the electrical resistivity along the main crystallographic directions. After a brief description of the experimental techniques in Sec. II, we present in Sec. III the experimental measurements performed. Finally, Sec. IV is devoted to the analysis and discussion of the results.

II. EXPERIMENTAL TECHNIQUES

The measurements presented in this paper were performed on several single crystals of $PrNi_5$ and $LaNi_5$

compounds, which were prepared by the Czochralski method in an induction furnace. For each compound a unique ingot has been subsequently spark cut in order to obtain three parallelepipeds with their sides perpendicular to the *a*, *b*, and *c* axes of the orthohexagonal cell, respectively. The typical dimensions of samples were $6\times1.5\times1.5$ mm^3.

The electrical resistivity in zero magnetic field was measured by an alternating-current four-probe method in the temperature range 1.5–300 K at the Laboratoire Louis Néel.

The measurements in magnetic fields, up to 22 T, were performed for different temperatures between 1.5 and 25 K in a Bitter coil at the Service National des Champs Intenses-Max Planck Institut of Grenoble. Here the electrical magnetoresistivity was measured by a standard four-terminal dc method. We measured longitudinal as well as transverse magnetoresistivity. "Longitudinal" means that the current and magnetic field are parallel. "Transverse" means that the electrical current and magnetic field are perpendicular. The residual resistivity ratios were about 10 for all samples.

III. EXPERIMENTAL RESULTS

The temperature dependences of the zero-field resistivity of $PrNi_5$ and $LaNi_5$ compounds are shown in Fig. 1 in the temperature range 1.5–300 K. One can see clearly the anisotropic behavior; in particular, the magnitude of the electrical resistivity along the *c* axis is lower than in the basal plane for both hexagonal compounds. The values of the residual resistivity ρ_0 are 4.70, 4.54, and 2.85 $\mu\Omega$ cm for $PrNi_5$ and 3.80, 3.95, and 2.29 $\mu\Omega$ cm for $LaNi_5$ along the *a*, *b*, and *c* axes, respectively. This anisotropy can be directly associated with that of the Fermi surface. It has been shown[10] that the ratio of the residual resistivities can be written as

$$\frac{\rho_{0a}}{\rho_{0c}}=\frac{\int_{E_F}dS_c}{\int_{E_F}dS_a}\ , \tag{1}$$

where $\int_{E_F}dS_u$ is the projection of the Fermi surface on the plane perpendicular to the *u*-axis. This ratio is about 1.7 for both $PrNi_5$ and $LaNi_5$, showing that we can expect similar Fermi surfaces for both compounds systems.[10]

From the $LaNi_5$ resistivity we have determined the Debye temperature $\Theta_D\cong230$ K. However, although the largest anisotropic contribution to the total electrical resistivity of the $PrNi_5$ compound comes from electron-phonon scattering, there is also another one which comes from the magnetic part of electrical resistivity. This explains the shoulder in the low-temperature region for $PrNi_5$ for the *a*, *b*, and *c* axes. In order to derive this latter contribution, we have subtracted the residual and phonon resistivities from the total resistivity of $PrNi_5$; the phonon part can be taken with very good approximation as equal to that of $LaNi_5$, and therefore,

$$\rho_{\rm mag}(T)=[\rho_{PrNi_5}(T)-\rho_{PrNi_5}(1.5\ {\rm K})]-[\rho_{LaNi_5}(T)-\rho_{LaNi_5}(1.5\ {\rm K})]\ . \tag{2}$$

The corresponding magnetic resistivities are shown in Fig. 2. In this picture we can see that the contributions along the *a* and *b* axes are larger than along *c* by about a factor 3. Note that this ratio is only approximative because it results from small differences between large resistivity values. The largest slopes take place in the temperature range 10–20 K, the maximum of the thermal derivative $d\rho_m/dT$ of the magnetic resistivity ρ_m occurring about 12 K for all directions. Note that at 40 K about 85% of the saturated value at 300 K is reached.

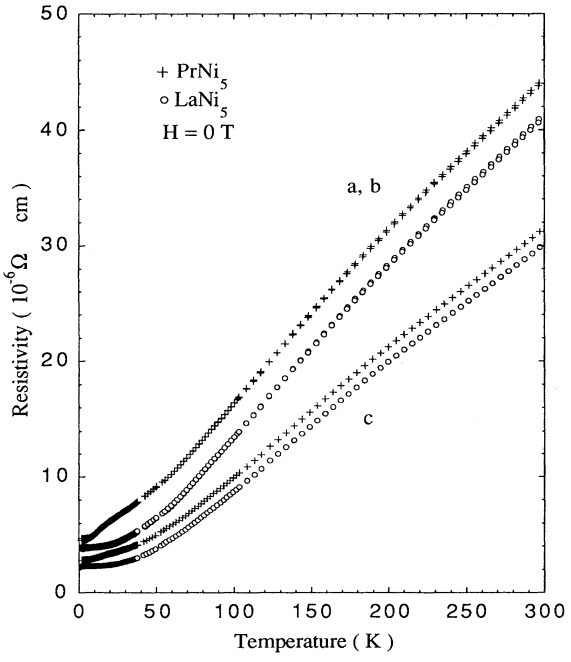

FIG. 1. Temperature dependences of the electrical resistivity of $PrNi_5$ and $LaNi_5$ in zero magnetic field.

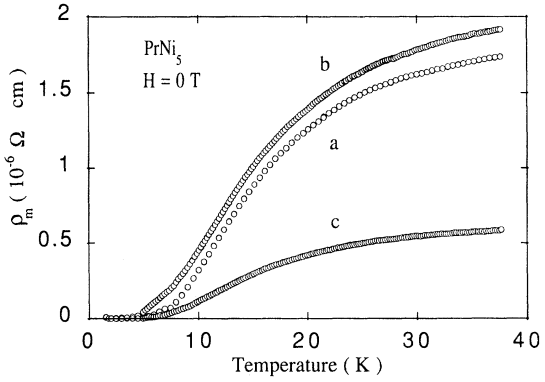

FIG. 2. Temperature dependences of the magnetic contribution ρ_m to the resistivity of $PrNi_5$.

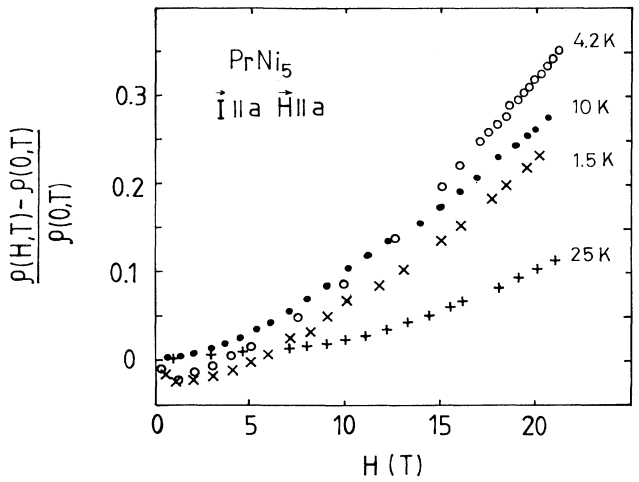

FIG. 3. Magnetic-field dependence of the electrical resistivity $[\rho(H,T)-\rho(0,T)]/\rho(0,T)$ when the current **I** and magnetic field **H** are parallel to the *a* axis (longitudinal *a*) at 1.5, 4.2, and 25 K.

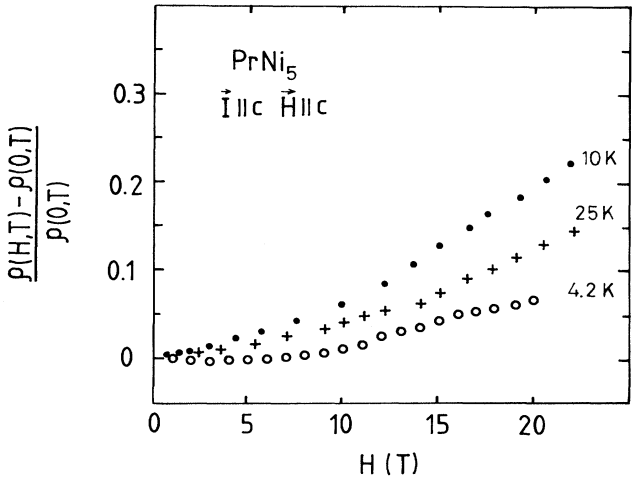

FIG. 5. Magnetic-field dependence of the electrical resistivity $[\rho(H,T)-\rho(0,T)]/\rho(0,T)$ when the current **I** and magnetic field **H** are parallel to the *c* axis (longitudinal *c*) at 4.2, 10, and 25 K.

In Figs. 3–5 we present the most characteristic results for longitudinal and transverse magnetoresistivities. The common feature for all the experimental data is that $\Delta\rho/\rho=[\rho(H,T)-\rho(0,T)]/\rho(0,T)$ increases with the magnetic field and decreases when the temperature T increases between 10 and 16 K, in agreement with the measurements on the polycrystalline sample.[7] Moreover, we do not observed any indication at $T=1.5$ K and up to 22 T for the effect of a crossover (metamagnetic transition) (Ref. 11) between the ground state and first excited CEF level along the *a* direction, which is a certain confirmation of the CEF-level scheme of $PrNi_5$ determined by point-contact-spectroscopy measurements in high magnetic fields.[9] Furthermore, all the dependences are proportional to H^n with $1.4\leq n\leq 2$. From Figs. 3 and 4 it is shown that $\Delta\rho/\rho$, when the current I is along the *a* axis (and also along the *b* axis), increases with temperature from 1.5 to 4.2 K and then starts to decrease, this variation being larger in the longitudinal case than in the transverse one when the current is along *a*. Nevertheless, in the longitudinal case with $\mathbf{I}\|c$ (see Fig. 5), this increase occurs at least up to 10 K. The small minimum which appears at 1.5 and 4.2 K in the longitudinal case with $\mathbf{I}\|a$ (see Fig. 3) is not yet understood.

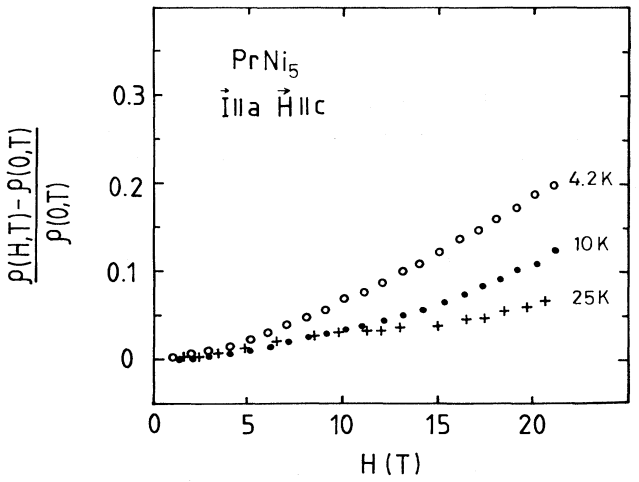

FIG. 4. Magnetic-field dependence of the electrical resistivity $[\rho(H,T)-\rho(0,T)]/\rho(0,T)$ when the current **I** is parallel to the *a* axis and the magnetic field **H** is parallel to the *c* axis (transverse *a*) at 4.2, 10, and 25 K.

IV. ANALYSIS AND DISCUSSION

Because $PrNi_5$ is paramagnetic, it is essential to start the analysis by using the SDR model,[12] which takes into account the scattering of conduction electrons by the disordered magnetic moments of Pr ions. The resulting resistivity can be expressed in the following compact form[13] for the current parallel to a unit vector **u**:

$$\rho^{\mathbf{u}}_{\mathrm{SDR}}=K^{\mathbf{u}}K_{\mathrm{SDR}}(g_J-1)\mathrm{Tr}(PQ)\ , \tag{3}$$

where $K^{\mathbf{u}}$ is a normalization factor common to all contributions to the resistivity, K_{SDR} contains the exchange coupling parameter between conduction and $4f$ electrons, and g_J is the Landé factor. The trace is taken over the different states of the system, and the symmetrical matrices P_{ij} and Q_{ij} are defined as follows:

$$P_{ij}=\frac{\exp(-E_i/k_BT)}{\sum_n \exp(-E_n/k_BT)}\ \frac{2}{1+\exp[(E_i-E_j)/k_BT]}\ , \tag{4}$$

where the first factor gives the population of the *i*th energy state and the second represents integrated Fermi factors. The indexes run over all the energy states obtained by diagonalizing the Hamiltonian $\mathcal{H}$ (see below). The second matrix

$$Q_{ij}=|\langle i|J_z|j\rangle|^2+\tfrac{1}{2}|\langle i|J_+|j\rangle^2+\tfrac{1}{2}|\langle i|J_-|j\rangle|^2 \quad (5)$$

contains matrix elements of the total angular momentum **J** between the states $|i\rangle$ and $|j\rangle$ of the system. This model can give rise to an anisotropy of the magnetic resistivity in zero field only through the dependence of K^{μ}, which is related to the band structure. Moreover, an additional anisotropy must occur according to the direction of the applied field, through the anisotropic splitting of the CEF states by the Zeeman term. The relevant Hamiltonian describing the magnetic properties of the $4f$ shell may be written using the equivalent-operator method[9] as

$$\mathcal{H}=\mathcal{H}_{\rm CEF}+\mathcal{H}_D+\mathcal{H}_Q \ . \quad (6)$$

In this expression,

$$\mathcal{H}_{\rm CEF}=B_2^0O_2^0+B_4^0O_4^0+B_6^0O_6^0+B_6^6O_6^6 \quad (7)$$

is the CEF Hamiltonian for hexagonal symmetry with the Stevens equivalent operators O_l^m and the CEF parameters B_l^m.[14] Within the molecular-field approximation, the second term in Eq. (6),

$$\mathcal{H}_D=-\mu_B g_J(\mathbf{H}+\lambda\mu_B g_J\langle\mathbf{J}\rangle)\cdot\mathbf{J} \ , \quad (8)$$

includes the Zeeman coupling and the isotropic bilinear Heisenberg-type exchange interaction. In this expression, **J** is the total angular momentum and λ is the molecular-field parameter acting on the Pr^{3+} ion corrected for the demagnetizating field and for the nickel contribution.[8] Finally, the last term, the two-ion quadrupolar Hamiltonian, can be written as

$$\mathcal{H}_Q=-G^{\alpha}\langle O_2^0\rangle O_2^0-G^{\varepsilon}\langle O_2^2\rangle O_2^2 \ , \quad (9)$$

where G^{α} and G^{ε} are the total quadrupolar coefficients. For our analysis we have used data given in Ref. 9, namely, $B_2^0=5.84$ K, $B_4^0=5.199\times10^{-2}$ K, $B_6^0=8.007\times10^{-4}$ K, $B_6^6=3.098\times10^{-2}$ K, $G^{\alpha}=-10$ mK, $G^{\varepsilon}=-20$ mK, and $\lambda=3.5\ T/\mu_B$.

The diagonalization of the Hamiltonian is carried out in a self-consistent manner. Using the SDR model, we are able to approximately describe our measurements in zero magnetic field only if $K^{\rm u}$ is 3 times less along c than along a and b (see Fig. 2). In Fig. 6 we compare the experimental data with the calculated variations of $d\rho_m/dT$. It is worth noting that the experimental maxima are observed at 12 K, whereas they are calculated at 14 K.

In order to emphasize the anisotropic contribution to the magnetoresistivity, we have reported in Fig. 7 the difference $\rho_{\parallel}(H,T)-\rho_{\perp}(H,T)$, where $\rho_{\parallel}$ ($\rho_{\perp}$) is the resistivity when magnetic field is parallel (perpendicular) to the current direction for the four conditions indicated in the figure caption. As shown by the calculated variations reported in Fig. 7, the SDR model, with the set of parameters determined above, is not able to explain, even qualitatively, the observed behaviors. Therefore, in the same way as quadrupolar interactions were introduced to describe the magnetic properties,[8] a quadrupolar contribution to the resistivity must be considered in order to give a better account of the observed data.

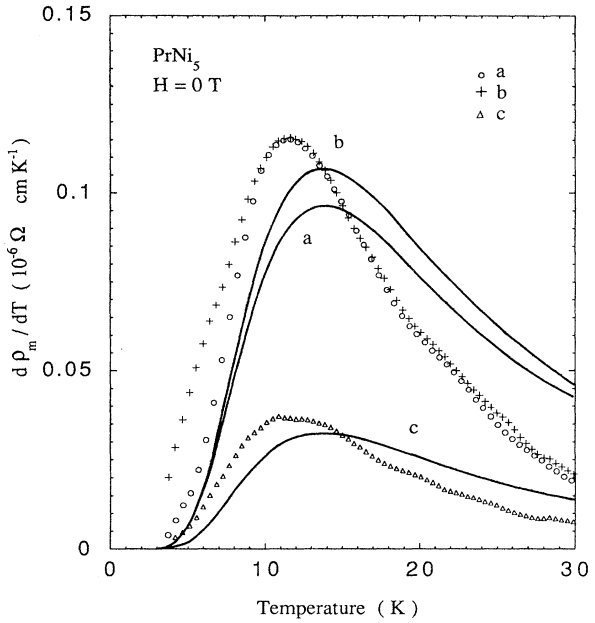

FIG. 6. Experimental and calculated temperature dependence of the derivative $d\rho_m/dT$ in zero magnetic field. Solid lines are the variations calculated with the SDR model for $K^a=0.9$, $K^b=1$, and $K^c=0.33$.

The theoretical model that we use has been extensively developed by Sablik and Levy[15] (and references therein). In this model the scattering mechanism comes mainly from the direct Coulomb scattering of conduction electrons by $4f$ aspherical charge distribution, and the quadrupole-disorder contribution to the resistivity is given as

$$\rho_Q^{\rm u}=K^{\rm u}\alpha_J^2\sum_Q(-1)^Q K_Q[\langle O^2_{-Q}(\mathbf{J};\mathbf{u})O_Q^2(\mathbf{J};\mathbf{u})\rangle_W - \langle O^2_{-Q}(\mathbf{J};\mathbf{u})\rangle\langle O_Q^2(\mathbf{J};\mathbf{u})\rangle] \ , \quad (10)$$

where $K^{\rm u}$ is the same as in Eq. (3), α_J is the Stevens multiplicative factor for the quadrupolar operators, $\langle A\rangle$ is the usual thermal average, and $\langle AB\rangle_W$ is the weighted thermal average defined by

$$\langle AB\rangle_W=\frac{1}{Z}\sum_{i,j}e^{-E_i/k_BT}\frac{(E_i-E_j)/k_BT}{1-\exp[(E_i-E_j)/k_BT]}\times\langle i|A|j\rangle\langle j|B|i\rangle \ . \quad (11)$$

$|i\rangle$ and $|j\rangle$ are the states defined before and Z is the partition function. The $O_Q^2(\mathbf{J};\mathbf{u})$'s are the spherical operators of rank 2, which are linear combinations of the usual Stevens equivalent operators $O_2^0, O_2^2, \ldots$. The notation used here emphasizes the fact that quadrupolar operators are quantized along the **u** direction of the current. Finally, the K_Q's are complicated combinations of $3j$ coefficients and radial integrals, which involve the character of the conduction electrons ($K_Q=K_{-Q}$) and in-

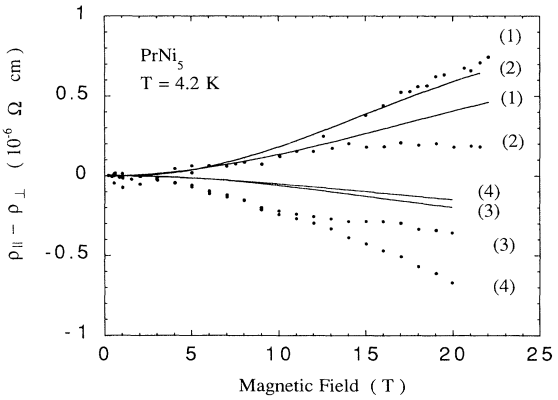

FIG. 7. Experimental and calculated magnetic field dependences at 4.2 K of (1) $\rho_{\parallel}(\mathbf{I}\|a,\mathbf{H}\|a)-\rho_{\perp}(\mathbf{I}\|a,\mathbf{H}\|c)$, (2) $\rho_{\parallel}(\mathbf{I}\|b,H\|b)-\rho_{\perp}(\mathbf{I}\|b,\mathbf{H}\|c)$, (3) $\rho_{\parallel}(\mathbf{I}\|c,H\|c)-\rho_{\perp}(\mathbf{I}\|c,\mathbf{H}\|b)$, (4) $\rho_{\parallel}(\mathbf{I}\|c,H\|c)-\rho_{\perp}(\mathbf{I}\|c,\mathbf{H}\|a)$. Solid lines are the variations calculated with the SDR model for $K^a=0.9$, $K^b=1$, and $K^c=0.33$.

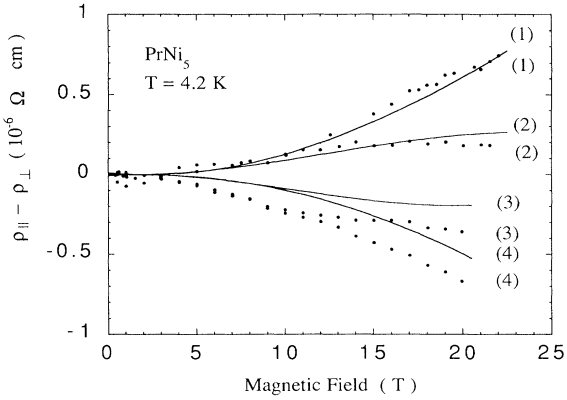

FIG. 9. Experimental and calculated field dependences at 4.2 K of $\rho_{\parallel}(H,T)-\rho_{\perp}(H,T)$. The labels used here are the same as those of the caption of Fig. 7. Solid lines are the variations calculated taking into account spin- and quadrupole-disorder contributions.

clude direct as well as exchange Coulomb contributions, the former one being predominant.[15,16]

This model [Eqs. (3) and (10)] has been used simultaneously to explain the thermal variations of ρ_m and field dependences of $\rho_{\parallel}(H,T)-\rho_{\perp}(H,T)$ at different temperatures. The best fit has been obtained with the following set of parameters: $K^a=0.95$, $K^b=1$, $K^c=0.65$, $K_{\mathrm{SDR}}=1.6\ \mu\Omega\,\mathrm{cm}$, $K_0=0.2\ \mu\Omega\,\mathrm{cm}$, $K_1=4.7\ \mu\Omega\,\mathrm{cm}$, $K_2=5.9\ \mu\Omega\,\mathrm{cm}$, $G^{\alpha}=-35$ mK.

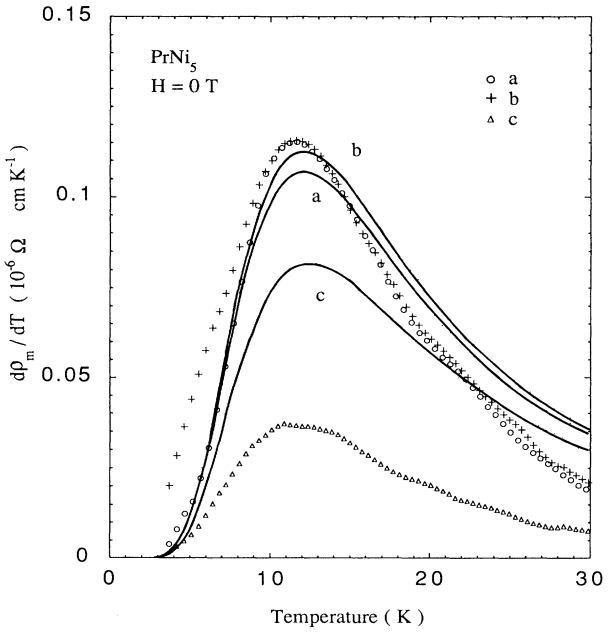

FIG. 8. Experimental and calculated thermal derivatives $d\rho_m/dT$ in zero magnetic field. Solid lines are the variations calculated taking into account spin and quadrupole-disorder contributions.

We have used $G^{\alpha}=-35$ mK in order to reduce the shift in temperature of the maximum of $d\rho_m/dT$. As shown in Figs. 8–10, these parameters improve noticeably all the fits. In particular, they account quite well for the measurements performed when the direction of the current is along the a and b axes. However, in the case of the c direction, these parameters describe only qualitatively the observed behaviors. From this analysis, the following features are noteworthy.

(i) Both spin-disorder as well as quadrupolar contributions to the resistivity are present. A similar result was obtained in $R\mathrm{Cu_2Si_2}$ compounds (R=rare earth), by comparison of resistivity measurements as functions of temperature, using spin only scattering of the Gd compound and the de Gennes factor as a guideline.[17]

(ii) The anisotropy of the electrical magnetoresistivity results in part from the anisotropy of the band structure

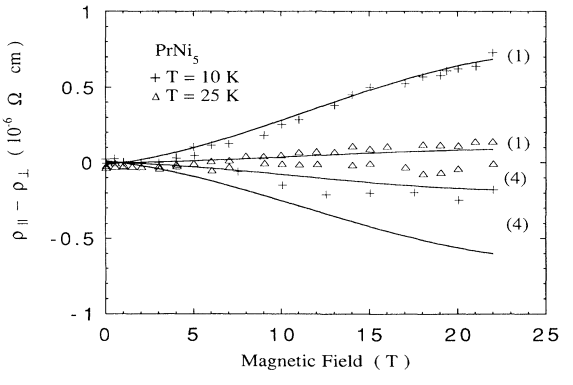

FIG. 10. Experimental and calculated field dependences at 25 K of $\rho_{\parallel}(H,T)-\rho_{\perp}(H,T)$ for the labels (1) and (4) of the caption of Fig. 7. Solid lines are the variations calculated taking into account spin- and quadrupole-disorder contributions.

through the K^u coefficients. Note that the deduced K^a/K^c ratio is close to ρ_{0a}/ρ_{0c}, which seems to be supported by the former assertion.

(iii) From our fits we have found that the quadrupolar parameter K_0 is one order of magnitude smaller than the other ones, K_1 and K_2. This means that the quadrupolar scattering itself is anisotropic (isotropy is obtained for $K_0=K_1=K_2$).

(iv) Finally, from the relative proportion of K_{SDR} and K_Q's, it turns out that the quadrupolar-disorder contribution to the total magnetic resistivity is about 5 times larger than the spin-disorder one. This fact shows that the quadrupolar scattering is the dominating one in $PrNi_5$.

In order to get a better knowledge of the anisotropy of the band structure, it would be worthwhile to perform de Haas–van Alphen experiments on these compounds. As well, it could be interesting to perform other types of transport measurements, such as thermal conductivity, in order to further investigate the influence of anisotropic quadrupolar scattering.

ACKNOWLEDGMENTS

We thank P. Lethuillier and J. C. Genna for their cooperation in the measurements performed at the Laboratoire Louis Néel. We acknowledge Professor P. Wyder for his stimulating interest in the subject.

*Permanent address: Facultad de Ciencias, Universidad de Cantabria, Santander, Spain.

[1]A. Fert and P. M. Levy, Phys. Rev. B **16**, 5040 (1977).
[2]A. Fert and P. M. Levy, Phys. Rev. B **16**, 5052 (1977).
[3]M. J. Sablik, P. Pureur, G. Creuzet, A. Fert, and P. M. Levy, Phys. Rev. B **28**, 3890 (1983).
[4]K. Andreas, S. Darack, and H. R. Ott, Phys. Rev. B **19**, 5475 (1979).
[5]K. Andreas and S. Darack, Physica (Utrecht) **86**, 107 (1977).
[6]M. Reiffers, K. Flachbart, S. Janos, A. B. Beznosov, and G. Eska, Phys. Status Solidi B **109**, 369 (1982).
[7]M. Reiffers and K. Flachbart, Jpn. J. Appl. Phys. **26**, Suppl. **3**, 439 (1987).
[8]V. M. T. S. Barthem, D. Gignoux, A. Nait-Saada, D. Schmitt, and G. Creuzet, Phys. Rev. B **37**, 1733 (1988).
[9]M. Reiffers, Yu G. Naidyuk, A. G. M. Jansen, P. Wyder, I. K. Yanson, D. Gignoux, and D. Schmitt, Phys. Rev. Lett. **62**, 1560 (1989).
[10]S. Legvold, in *Magnetic Properties of Rare Earth Metals,* edited by R. J. Elliot (Plenum, New York, 1972), Chap. 7.
[11]E. Leyarovski, J. Mrachkov, A. Gilewski, and T. Mydlarz, Phys. Rev. B **35**, 8668 (1987).
[12]V. U. S. Rao and W. E. Wallace, Phys. Rev. B **2**, 4613 (1970).
[13]N. H. Andersen, P. E. Gregers-Hansen, E. Holm, H. Smith, and O. Vogt, Phys. Lett. **65A**, 1321 (1974).
[14]K. H. J. Stevens, Proc. Phys. Soc. London A **65**, 209 (1952).
[15]M. J. Sablik and P. M. Levy, J. Appl. Phys. **49**, 2171 (1978).
[16]D. Schmitt and P. M. Levy, J. Magn. Magn. Mater. **49**, 15 (1985).
[17]E. Cattaneo and D. Wohlleben, J. Magn. Magn. Mater. **24**, 197 (1981).